AFRL-RW-EG-TR-2009-7080

POSITRONIUM ANNIHILATION GAMMA RAY LASER

Allen P. Mills, Jr.

Physics Department
University of California
Riverside, CA 92521

GRANT NO. FA8651-07-1-0003

JULY 2009

FINAL REPORT FOR PERIOD APRIL 2007 - APRIL 2009

AIR FORCE RESEARCH LABORATORY, MUNITIONS DIRECTORATE

■ **Air Force Materiel Command** ■ **United States Air Force** ■ **Eglin Air Force Base**

STINFO COPY

NOTICE AND SIGNATURE PAGE

Using Government drawings, specifications, or other data included in this document for any purpose other than Government procurement does not in any way obligate the U.S. Government. The fact that the Government formulated or supplied the drawings, specifications, or other data does not license the holder or any other person or corporation; or convey any rights or permission to manufacture, use, or sell any patented invention that may relate to them.

This report was cleared for public release by the 96 Air Base Wing, Public Affairs Office, and is available to the general public, including foreign nationals. Copies may be obtained from the Defense Technical Information Center (DTIC) <http://www.dtic.mil/dtic/index.html>.
.

AFRL-RW-EG-TR-7080 HAS BEEN REVIEWED AND IS APPROVED FOR PUBLICATION IN ACCORDANCE WITH ASSIGNED DISTRIBUTION STATEMENT.

FOR THE DIRECTOR:

//ORIGINAL SIGNED//	//ORIGINAL SIGNED//
Dr. Azar Ali	Lt. Aaron Doyle
Technical Director	Program Manager

This report is published in the interest of scientific and technical information exchange, and its publication does not constitute the Government's approval or disapproval of its ideas or findings.

STINFO COPY

REPORT DOCUMENTATION PAGE

Form Approved
OMB No. 0704-0188

1. REPORT DATE *(DD-MM-YYYY)*	2. REPORT TYPE	3. DATES COVERED *(From - To)*
30-07-2009	FINAL	April 2007 - April 2009

4. TITLE AND SUBTITLE
POSITRONIUM ANNIHILATION GAMMA RAY LASER

5a. CONTRACT NUMBER
N/A

5b. GRANT NUMBER
FA8651-07-1-0003

5c. PROGRAM ELEMENT NUMBER
62602F

6. AUTHOR(S)
Allen P. Mills, Jr.

5d. PROJECT NUMBER
2502

5e. TASK NUMBER
99

5f. WORK UNIT NUMBER
25

7. PERFORMING ORGANIZATION NAME(S) AND ADDRESS(ES)

Physics Department
University of California
Riverside, CA 92521

8. PERFORMING ORGANIZATION REPORT NUMBER

9. SPONSORING / MONITORING AGENCY NAME(S) AND ADDRESS(ES)
AFRL/RWAV
101 W. Eglin Blvd. Bldg 13
Eglin AFB, FL 32542-6810

10. SPONSOR/MONITOR'S ACRONYM(S)
AFRL-RW-EG

11. SPONSOR/MONITOR'S REPORT NUMBER(S)
AFRL-RW-EG-TR-2009-7080

12. DISTRIBUTION / AVAILABILITY STATEMENT
DISTRIBUTION A: **Approved** for public release; distribution unlimited. 96th ABW/PA Approval and Clearance # 96ABW-2009-0370, dated 31 Aug 2009

13. SUPPLEMENTARY NOTES
AVAILABILITY OF THIS REPORT IS SHOWN ON THE NOTICE PAGE. DISTRIBUTION INDICATING AUTHORIZED ACCESS IS ON THE COVER PAGE AND BLOCK 12 OF THIS FORM.

14. ABSTRACT
The goal of the work reported here is the perfection of a powerful laser based on the coherent annihilation of a Bose-Einstein condensate of positronium, the hydrogen-like atoms formed from bound electron-positron pairs. We have made progress in several areas that takes us closer to our goal. Specifically we report (I) advances in positron storage and manipulation techniques; (II) Development of laser systems for cooling positronium atoms and measuring their velocity distribution; (III) A theoretical estimate of the ignition threshold for DT fuel heated by a burst from an annihilation gamma ray laser; and (IV) A new concept for more rapid laser cooling of light atoms including positronium.

15. SUBJECT TERMS
Fusion, Bose Einstein Condensate (BEC), power, laser, positron storage, positronium storage

16. SECURITY CLASSIFICATION OF:			17. LIMITATION OF ABSTRACT	18. NUMBER OF PAGES	19a. NAME OF RESPONSIBLE PERSON
a. REPORT	b. ABSTRACT	c. THIS PAGE			Lt. Aaron Doyle
UNCLASSIFIED	UNCLASSIFIED	UNCLASSIFIED	UL	42	19b. TELEPHONE NUMBER *(include area code)*

STINFO COPY

Standard Form 298 (Rev. 8-98)
Prescribed by ANSI Std. Z39.18

REPORT DOCUMENTATION PAGE

ABSTRACT

The goal of the work reported here is the perfection of a powerful laser based on the coherent annihilation of a Bose-Einstein condensate of positronium, the hydrogen-like atoms formed from bound electron-positron pairs. We have made progress in several areas that takes us closer to our goal. Specifically we report (I) advances in positron storage and manipulation techniques; (II) Development of laser systems for cooling positronium atoms and measuring their velocity distribution; (III) A theoretical estimate of the ignition threshold for DT fuel heated by a burst from an annihilation gamma ray laser; and (IV) A new concept for more rapid laser cooling of light atoms including positronium.

TABLE OF CONTENTS

LIST OF FIGURES

LIST OF TABLES

ACKNOWLEDGEMENT

The PI would like to acknowledge Mr. Ken Edwards,
whose far-sighted vision supported our beginning work on the annihilation gamma ray laser.

SUMMARY

This report gives the results obtained under a two year RevTek grant on the topic of Revolutionary Technology for Energy Sufficiency. The idea being explored is to use an annihilation gamma-ray laser to enable ignition of a fusion burn for actinide-free production of energy.

A practical fusion energy source is the only way to energy sufficiency for the United States of America that will eliminate the strangle-hold of foreign oil. The three approaches presently on the table are close to scientific break even, but are far from being practical. Plasma fusion occurs at such low densities that the experimental reactor has grown too large to be competitive. Laser fusion obtains very high fuel densities but requires the use of laser powers that do not seem to be scalable. The impact fusion concept proposes to create high densities with high speed projectiles, but so far the densities that can be achieved are not sufficient to initiate burn.

A possible solution would be to use a gamma ray laser to initiate burn in fuel that has been compressed via shock compression. The advantage over the use of x-ray lasers is that the superior penetrability of annihilation gammas would allow penetration of higher atomic number materials used for compression.

A prerequisite for the gamma laser is generating and controlling a large number of positrons at high density. We have made progress in this area by improving our positron beam to produce dense pulses of positrons such that we were able to produce the first dipositronium molecules.

The positrons for a laser would have to be in the form of positronium that has formed a Bose-Einstein condensate. Achieving this state will require improved laser diagnostics and we report here the development of cooling and measuring laser systems that will be needed for this task.

To have an idea whether the proposed laser ignited fusion might be practical, we have made a preliminary estimate of the threshold conditions for initiating ignition of a DT fusion burn. At ten times liquid density the threshold would occur for 0.5 MJ energy deposited at the center of a spherical fuel pellet, corresponding to the energy that would be obtained from the annihilation of about 10^{19} positrons. While this is about one billion times as many as the record number of stored positrons, there is as yet no reason why it should not be possible to develop the technology to this point.

When such large numbers of positronium atoms are used, the critical temperature for Bose-Einstein condensation will be higher than room temperature. However, at the early stages where the underlying physics is being established, we will probably be necessary to use laser cooling to achieve a positronium Bose-Einstein condensate. Since positronium only lives for a few hundred nsec while it is being cooled, it is essential that the cooling be as efficient as possible. With this in mind, we have invented and report here a new method for cooling positronium that should allow us to cool from a four times higher starting temperature.

INTRODUCTION

This report gives the results obtained under a two year RevTek grant on the topic of Revolutionary Technology for Energy Sufficiency. The idea being explored is to use an annihilation gamma-ray laser to enable ignition of a fusion burn for actinide-free production of energy.

Summary Concept

A practical fusion energy source is the only way to energy sufficiency for the United States of America that will eliminate the strangle-hold of foreign oil. The three approaches presently on the table are close to scientific break even, but are far from being practical. Plasma fusion occurs at such low densities that the experimental reactor has grown too large to be competitive. Laser fusion obtains very high fuel densities but requires the use of laser powers that do not seem to be scalable. The impact fusion concept proposes to create high densities with high speed projectiles, but so far the densities that can be achieved are not sufficient to initiate burn.

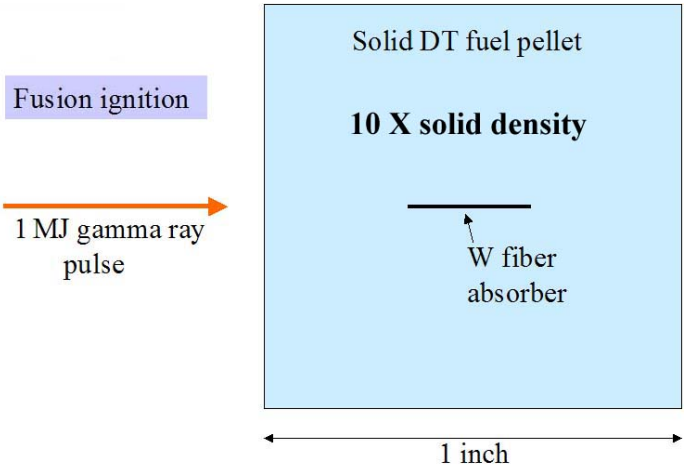

Figure 1. Ignition of a 1 inch DT fuel pellet at 10 x solid density using a 1 MJ gamma ray laser pulse.

The PI proposed reviving the impact fusion concept by using an annihilation gamma ray laser to ignite a fusion reaction in a compressed DT target, as indicated in Figure 1. The cubic inch of compressed DT shown in Figure 1 would burn in about 1 ns to yield 1,000 GJ of energy, ten times the current engineering break-even value. The process can be repeated every 1000 sec to yield a 1 GW reactor as indicated in Figure 2 or a single DT detonation could be used to set off a 1 megaton blast using a cubic meter of liquid D_2.

Figure 2. Power plant concept using periodic explosions of small DT pellets.

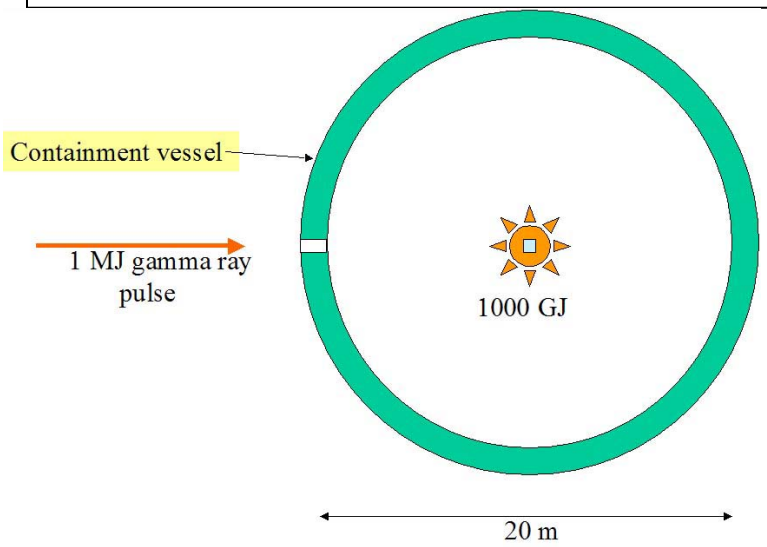

Goals: The ultimate aim of the work I propose here is to perfect a powerful laser based on the coherent annihilation of a Bose-Einstein condensate of positronium [[1]], the hydrogen-like atoms formed from bound electron-positron pairs. Because this approach is beyond the present state of the art, I am proposing here to begin work by (i) building up the components needed for obtaining and manipulating significant quantities of antimatter, (ii) making the first experimental positronium annihilation gamma ray lasers and (iii)

making substantial increases in our technical capabilities for using antimatter. The specific goals are:

- Form a Bose-Einstein condensate of spin-polarized triplet positronium atoms, which is a prerequisite for making an annihilation gamma ray laser, and observe its properties.
- Develop the necessary antimatter technology components including a positron storage device for storing and delivering 10^{13} positrons in a single 100 ns burst.
- Observe the stimulated emission of annihilation gamma rays which is the precursor to lasing.
- Make a positronium annihilation gamma ray laser delivering 1 Joule gamma ray pulses.
- Increase the positron storage to 10^{16} positrons and the laser energy to 1 kJ.
- Assess the prospects for scaling the technology to a system capable of delivering 1 MJ annihilation gamma ray laser pulses from a few nano-grams of positronium (10^{19} atoms).

Potential contribution to the Air Force. A powerful annihilation gamma ray laser could be used (1) as a clean igniter of fusion reactions both for energy production and for explosive devices and (2) to supply a large dose of gamma rays that would render a distant threatening object ineffective. For the latter type of applications above the earth's atmosphere, a substantial fraction of the energy of a small fusion device would be converted into a collimated beam of annihilation photons that would propagate through space and intercept the object. For power production, the positrons would be produced by conventional means via particle accelerators and stored in an accumulator for eventual use. Successful implementation of clean fusion for power production would be one of the major breakthroughs hoped for this millennium, and would nullify oil's present stranglehold to the obvious advantage of the United States of America. There are many potential roadblocks on the path to such a capability and I propose to find out as quickly as possible whether the approach is practical and cost effective by a serious program demonstrating the first positronium annihilation gamma ray lasers.

Proposed technical approach. The annihilation of the electron and positron in a singlet positronium atom produces a pair of 511 keV photons. A collection of singlet positronium atoms of sufficient density and low enough thermal motion may be induced to annihilate coherently and thus form the basis for a gamma ray laser. [See Figure 3.] Assuming the implementation of only modest technical advances, we have the knowledge to make an annihilation laser capable of operating above the few mJ per pulse threshold level. To make a useful annihilation laser system capable of delivering 1 MJ of gamma ray energy to a 1 mm^2 target area at a distance of 100 m we need enormous technical developments in positron production, confinement, long-term storage and manipulation. I propose to explore the practicality of an annihilation laser by making the first lasers ever to be based on antimatter, by increasing the positron

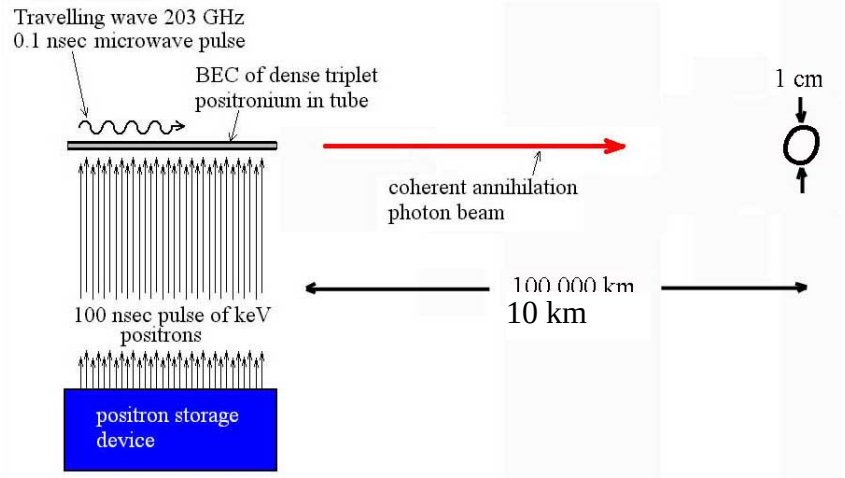

Figure 3. Annihilation laser concept. Positrons from a storage device are suddenly deposited in a tube several centimeters long and a few microns in diameter. The positrons form triplet positronium atoms that quickly cool to a few thousand degrees C and form a Bose-Einstein condensate. A microwave burst converts the positronium to the singlet state and a spontaneous annihilation photon that happens to propagate along the tube is amplified via stimulated emission to form a powerful coherent beam of annihilation photons.

production rate using a high energy accelerator and by making vastly improved traps for collecting and storing positrons.

Advantages of the proposed approach. The advantages of photons with energies of several hundred keV, loosely termed "gamma-rays", over optical energy photons for inflicting damage on a distant target or for igniting fusion reactions are:

- Gamma rays penetrate a target to a thickness of roughly 10 g/cm^2 and so impart up to two orders of magnitude greater impulse for a given energy compared to visible or infrared photons, thus leading to the fissure of large objects.
- Gamma rays are not significantly deflected by the atmosphere or its fluctuations, although absorption by the air limits the range at sea level to approximately 100 m if no means if employed for making a transparent gamma-ray channel through the atmosphere.
- The small size of the gamma-ray laser would be advantageous for steering and portability.
- A small annihilation gamma-ray laser would be fuelled by stored antimatter (positrons), which would leave no trace of radioactivity, although a GJ device might need to be based on energy derived from fusion.

Suitability of the PI for this project. The Pi is one of the world's best experimenters with positrons and has forty years of proven innovation in the field.

Plan of work. The first annihilation laser will be made in the following steps:

1. Attain Bose-Einstein condensed (BEC) positronium.
2. Make a source capable of delivering 10^{12} slow positron per second on a 1 mm target.
3. Develop a multiple trap for storing and releasing 10^{13} positrons.
4. Observe stimulated annihilation.
5. Make 1J annihilation gamma ray laser pulses.

A three year project to get through step 1 would proceed via the following tasks.

A. Year 1: Make a system for producing brightness enhanced 10 ns pulses of 10^7 5 keV positrons in a 10 μm diameter spot.

B. Year 1: Develop a method for making cavity structures in porous silica for containing BEC positronium.

C. Year 2: Make a BEC positronium target chamber with 4K cooling and optical access.

D. Year 3: Develop a laser system for detecting the BEC state via the disappearance of Doppler broadening.

E. Year 3: Characterize the positronium BEC by measuring the condensate fraction as a function of time, temperature and density.

One will note that each of the steps will be exploring interesting physics with the possibility of unexpected results and important technological applications, including for example (a) study of the time structure of a positron initiated thermite reaction, (b) measurement of Ps thermalization and diffusion dynamics, (c) observation of the giant absorption cross section associated with a coherent state localized within an optical wavelength. The first positronium BEC will be remarkable for its high critical temperature and quasi 2D behavior which will be evident in the condensate density as a function of temperature.

METHODS and PROCEEDURES

We have used a small laboratory positron apparatus and optical laser setup to make progress towards our goal of making an annihilation gamma ray laser by improving our ability to produce dense collections of positrons through direct experiment, beam transport simulations, target chamber development, and laser development.

The production of intense positron pulses for studies of interacting positronium atoms is now beginning its seventh year. This work is primarily funded by the National Science Foundation, but due to the pioneering nature of the work, and the concurrent need to develop new methodologies and instrumentation, obtaining data has taken a long time; without the Air Force contribution much of what has been achieved would not have been possible, or would at least have taken significantly longer.

We have succeeded in observing spin exchange quenching of the long o-Ps lifetime due to Ps-Ps collisions in a dense collection of positronium (Ps) in a porous target [2] and have obtained evidence for the first observation of the di-positronium molecule, Ps_2 [3]. This has been made possible by the development of a new positron bunching arrangement. By accumulating many positrons in a Surko-type trap [4] and performing certain manipulations upon the resulting plasma we have been able to generate positron bursts with spatio-temporal densities sufficiently high to allow us to observe interactions between Ps atoms. The development of the positron accumulator along with a pulsed magnet system and a buncher (see Figure 4) has allowed us to produce intense pulses with an instantaneous positron current of up to 10 mA [5**Error! Bookmark not defined.**]. We have also developed the new technique of "single shot positron annihilation lifetime spectroscopy" (SSPALS) [6] which makes it possible to observe short-lived interactions between positronium atoms.

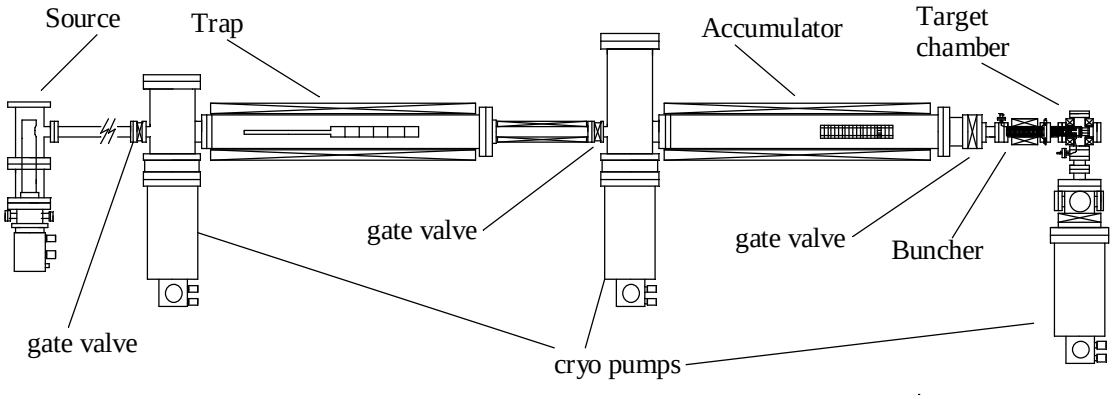

Figure 4. The first generation UCR positron accumulator. A rare gas moderator and source based beam supplies a gas filled trap which in turn delivers positrons to a UHV accumulator. After collecting the desired number of positrons in the accumulator they are compressed spatially using a "rotating wall" electric field and then ejected with a 200V pulse which compresses them temporally. A second time-bunching voltage is applied to the traveling positron plasma that compresses the pulse to a sub-nanosecond time width, and a 2 Tesla magnet around the target further compresses the beam spatially. This allows sub ns pulses with areal densities up to 5×10^{10} cm^{-2} to be delivered to the target region every few minutes.

Molecular positronium was created and observed by implanting intense positron bursts into a porous film and measuring a change in the Ps lifetime (the quenching signal) as a function of the beam density and sample temperature. Since Ps_2 formation requires a third body only Ps atoms in a surface state are able to form the molecule. Thus by desorbing the atoms from this state by heating the sample we observe

simultaneously an increase in the amount of long lived Ps present (f_d) and a decrease in the quenching signal *Q*, as shown in Figure 5. We have also observed some evidence for the formation of Ps_2 on a metal surface [7].

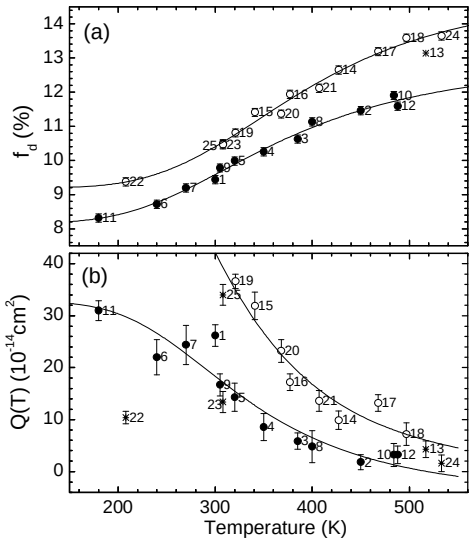

Figure 5. Temperature dependence of f_d and Q. a, f_d (the positronium fraction) as a function of temperature measured using a beam density of 0.9 x 10^{10} cm^{-2}. b, Q (the quenching signal) as a function of temperature. The inverse correlation of these two signals is strong evidence for the formation of Ps_2 formation on the internal surfaces of the porous silica.

Until our results there had been no previous experimental studies of many Ps systems at all [8]. Indeed, even though the positron was first observed in 1933 [9], Ps in 1951 [10] and the positronium negative ion in 1981 [11], the Ps_2 molecule (which is the next member of the polyelectron series envisioned by Wheeler [12] was only recently observed, because the required high positron densities were not available. Nevertheless, while convincing, the data shown in Figure 5 constitute an *indirect* observation of Ps_2. In order to make a definitive observation, and indeed to study the molecule and measure its lifetime and energy levels it will be necessary to substantially increase the available signal and conduct laser spectroscopy. This means increasing the positron beam density and developing the required laser systems.

RESULTS AND DISCUSSION

I. Positron beam Modifications

The experiments described above were all conducted using a pulsed magnet to compress the beam to an areal density ~ 5 $\times 10^{10}$ cm^{-2}, which was sufficient to produce a signal but, at least in the case of Al(111) only barely so. For Ps_2 production in vacuum it is desirable to use a clean metal surface, and since this is essential for laser spectroscopy of the molecule we should like to increase the positron beam density, and hence the Ps_2 production rate. Similarly, the production of a Ps BEC requires a density increase of three (or more) orders of magnitude over our previous work. For this reason our recent efforts have been focused on upgrading the positron beam to increase the density. We have done this in two ways: increasing the positron plasma compression in the accumulator and remoderating [13] the positrons in a field free region.

Plasma compression

The use of the "rotating wall" technique allows us to compress positron plasmas prior to releasing them from the accumulator, and in effect makes it possible to "dial up" a required density (within a certain range). In principle the plasma density should increase linearly with the applied rotating wall frequency, f_{RW}, so long as the plasma is actually rotating at this frequency. That is, if the plasma E × B frequency, f_{ExB} is the same as f_{RW}. This condition is known as the "no slip" or strong drive regime. The E × B rotation frequency is related to the plasma frequency, f_p, and the cyclotron frequency, f_c, via the relationship

$$f_{ExB} = \frac{f_p^2}{2 f_c} \approx C \frac{n_P}{B} \qquad (1)$$

Here n_p is the positron plasma density (cm^{-3}), B is the axial magnetic field strength (kG) and C is 0.0145. For a fixed magnetic field we see from eqn (1) that in the strong drive regime the plasma density should increase linearly with the applied rotating wall frequency. This is in fact what we observe, but only over a limited frequency range. This was not previously understood but recently we have increased the frequency range by the use of correction coils, as explained below.

The compression of plasmas by the application of a rotating wall electric field is affected by other factors, including plasma heating and the excitation of various plasma modes. In a high field trap plasma cool by the emission of cyclotron radiation, whereas in a weak magnetic field such as we use a cooling gas must be used (SF_6 in this case). This actually makes possible an additional heating mechanism. Particle scattering with gas molecules across the electric field lines leads to joule heating, and is enhanced at higher densities, which could mean that there is a limit to the amount of cooling possible. At the gas densities we have been using (~ 1 × 10^7 Torr) the total cooling rate should be comparable to that obtained via cyclotron radiation. The excitation of a zero frequency mode (ZFM) can strongly influence positron plasma compression. These modes are excited in the plasma when a static asymmetry becomes resonant with the rotating plasma, and therefore depend on the rotation frequency. These ZFM resonances were discovered by Surko et al, who showed that in the strong drive regime it is possible to either bypass the resonances or simply drive through them and continue to compress the plasma. However, on resonance ZFM's lead to strong plasma heating and loss of compression if there is insufficient cooling.

We have found, working with Rod Greaves of First Point Scientific Incorporated (FPSI), that using correction coils it is possible to cancel out some of the static asymmetries that lead to ZFM's, which significantly increases the plasma compression that may be obtained. Figure 6 shows the positron plasma central density as a function of the compression frequency applied to the rotating wall electrodes. It is

clear from the figure that not only do the correction coils allow the plasma to stay in the strong drive regime over a much larger frequency (and thus density) range, but that the existence of ZFM's do not necessarily prevent plasma compression from operating. At ~ 12 MHz there is an abrupt loss of compression whose nature is not yet fully understood. It is possible that at higher densities there exist many overlapping ZFM resonances that overlap to form a quasi-continuum (ass opposed to the discrete resonances seen at lower frequencies). Another possibility has been suggested by Cliff Surko in which the balance between heating and cooling provided the SF_6 gas has an upper density limit, after which the heating wins in a runaway process. If this is the case then it is unlikely that anything can be done to increase the plasma density beyond this limit. On the other hand, if the loss is caused by ZFM resonances then better field alignment should mitigate this effect. Work is underway to investigate this matter.

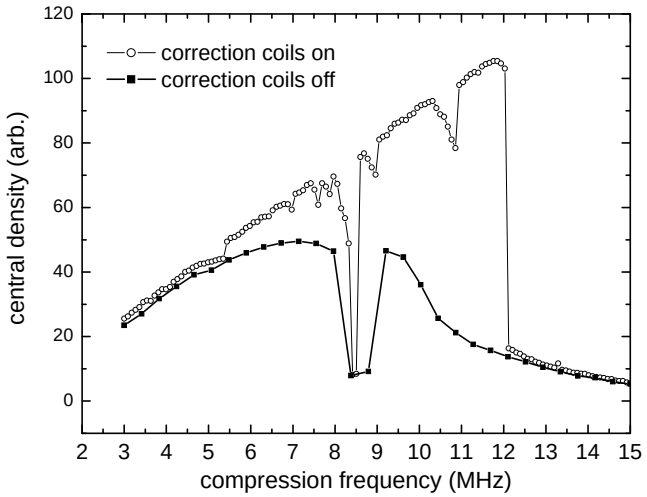

Figure 6. The plasma density increases linearly with the rotating wall compression frequency, indicating that the system is in the strong drive regime. When the correction coils are applied the frequency range over which this occurs is greatly increased, which allows us to achieve more than a factor of two higher densities than had previously been the case. We can also see that ZFM interruptions do still occur, but they are much less disruptive and can in general be overcome or avoided.

In addition to using correction coils we have also found that the highest plasma densities can only be obtained if there are a sufficient numbers of particles present in the accumulator. The reason of this is simply that if there are too few particles then the corresponding plasma density for some frequency can require that the radius be much lower than the plasma Debye length. In this case the particles will not respond collectively, and plasma effects, of which the RW compression is an important example, will not occur. The reason why this depends on the total number of particles N_p rather than the plasma density n_p is simply that both the Debye length λ_D and the radius r_p depend on the square root of the density. This means that during plasma compression the ratio of these parameters does not change. That is,

$$\lambda_D = \left(\frac{kT}{4\pi e^2 n_p} \right)^{1/2} = \left(\frac{kT\pi r_p^2 L_p}{4\pi e^2 N_p} \right)^{1/2} . \qquad (2)$$

Thus, if the plasma length L_p is constant (as it virtually is in a square well) we have

$$N_p / C_1 T = \left(r_p / \lambda_D \right)^2 \qquad (3)$$

Where C_1 is ~ 1.2 × 10^7 for a 7 cm long well (T = plasma temperature in eV, which we assume is constant). Compression requires that $r_p > \alpha\lambda_D$ (where α is some number that essentially defines when the system is in a plasma state) there will be some value of N_p below which the condition $\alpha > 1$ is not met. This effect is evident in Figure 7. There is obviously not a sharp transition into a plasma state, partly because the plasma density distribution is non-uniform, but also because partial Debye shielding will begin to occur as α increases.

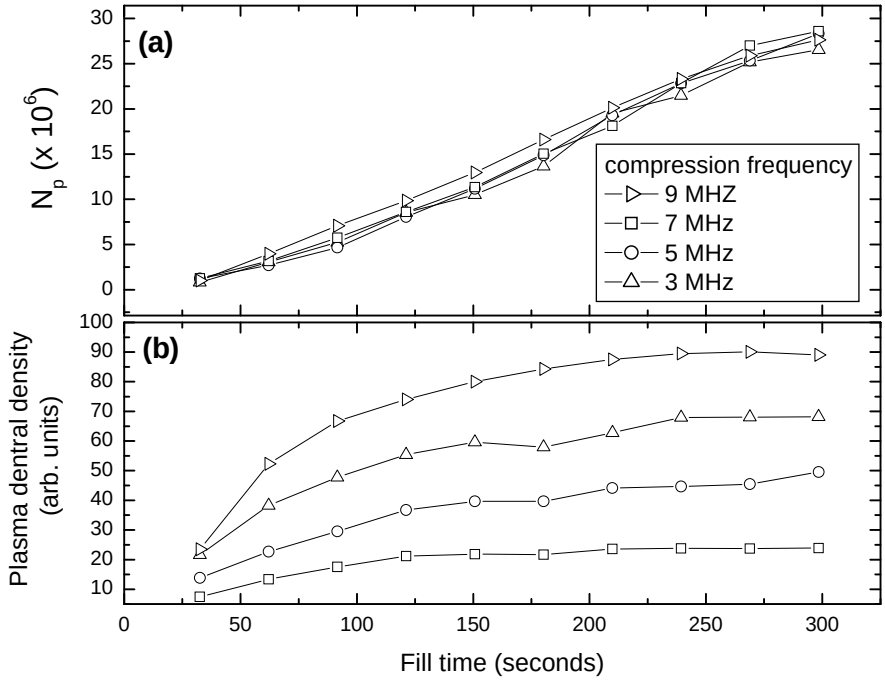

Figure 7 The applied RW frequency compresses plasmas in the strong drive regime according to eqn (1), but only if the density is sufficiently high to allow the particles to behave collectively (i.e., the positron cloud must be in a plasma state). When the total number of particles is too low the compression for a given frequency will be halted as the plasma is compressed at some density that is less than would be expected for a given frequency, as shown in the figure. The top panel (a) shows that the total number of positrons is essentially constant for a given fill time regardless of the plasma density. The lower panel (b) shows that as the number of positrons in the accumulator is increased the compression tends towards a frequency dependent limit. This tells us that there is a minimum number of positrons per pulse required in order to optimize the final plasma density.

Beam Remoderation

Although positron beam remoderation has been demonstrated many times this type of brightness enhancement has never been applied to intense pulses obtained from an accumulator. In most respects the methodology is expected to be the same as that used for DC beams. The main differences come from the fact that positrons must be extracted from the magnetic field of the accumulator, and that the use of a buncher leads to a large energy spread, which adversely affects the electrostatic focusing.

The modified beam system has been constructed and is shown in Figure 8. The source, trap and accumulator sections are identical to those shown in Figure 4 (except we have added correction coils, as described above). The magnetic field is maintained up to the end of the buncher where it is abruptly terminated by a mu-metal enclosure with a 3 mm diameter hole. As the beam exits this hole the radial expansion is countered by an electrostatic lens that focuses the beam onto a thin (100 nm) Ni foil. This

process dramatically increases the transverse energy of the beam, but this enery is dissipated in the remoderating foil, and the ~ 10% of the beam that emerges from the other side may then be transported in a field free region and refocused onto the target. In this way we expect to be able to produce a beam spot containing around 3 million positrons in a 25 micron FWHM spot, corresponding to an areal density of ~ 5×10^{11} cm^{-2}, which is an order of magnitude higher than we have obtained previously.

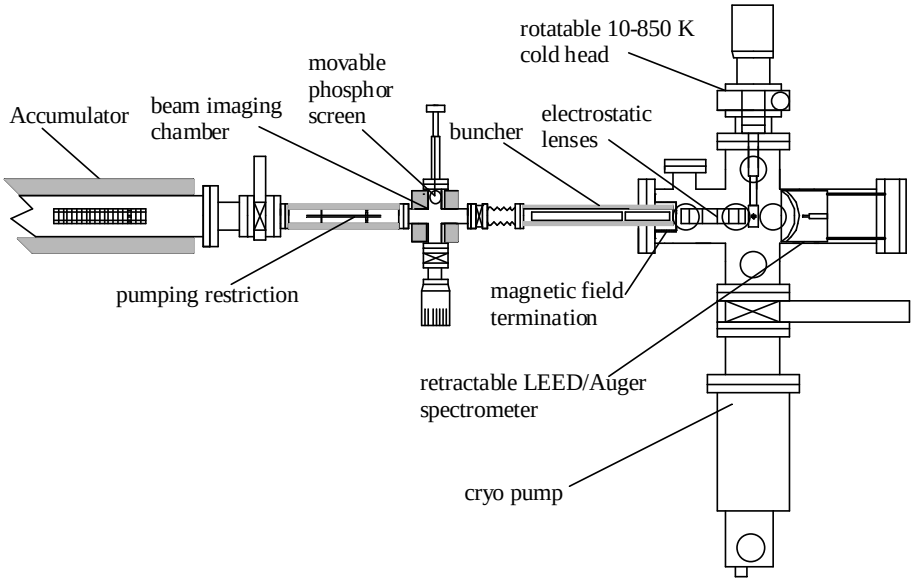

Figure 8 The new system allows us to extract the positron beam from the magnetic field and remoderate. Then the beam is electrostatically transported and focused onto the target. Although this involves a loss of around 90% of our positrons, the beam density is expected to be substantially increased.

Work is still in progress to produce the electrostatic pulsed beam. The estimate of the spot size is a conservative one based on simulations that are described in detail below. So long as space charge effects are not significant it may be possible to do much better, and a spot size of 5 microns is not out of the question (corresponding to a beam areal density of ~ 1×10^{13} cm^{-2}). This, however, will probably require a new lens design to optimize filling and minimize aberrations. This will be necessary for future Ps BEC experiments, but for the Ps_2 spectroscopy a spot size smaller than 50 microns will probably be sufficient.

So far we have successfully extracted the positron beam from the magnetic field and focused it with the first lens. Figure 9 shows beam profiles measured before and after extraction from the field. Although it is difficult to measure exactly how much beam is lost by taking it out of the field the fact that the pulse shape is hardly different before and after indicates that most of the beam is being transported.

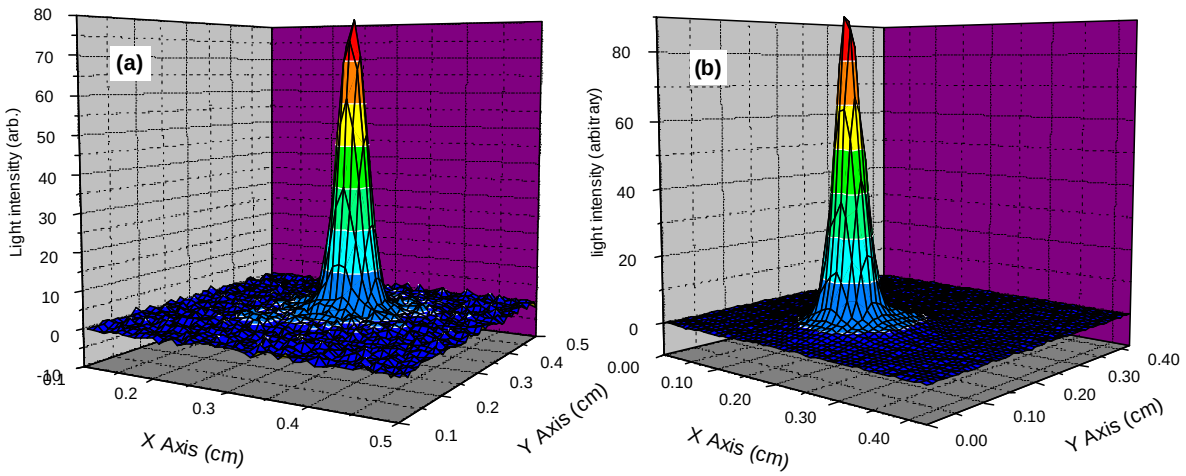

Figure 9 Positron beam profiles measured in the imaging chamber (a) just after the accumulator (in an axial magnetic field of ~ 700 Gauss) and on a phosphor screen placed in the position of the remoderator foil (b) where the field is essentially zero.

Electrostatic Lens Simulations

The expected system performance has been calculated using numerical simulations from commercial software packages. The beam focus onto the target is obtained in two phases. In a first phase the positron beam is extracted from the magnetic field and focused onto a thin Nickel foil where the positrons subsequently thermalize and are re-emitted on the other side of the foil with about 1 eV energy. In a second phase the now well defined beam is further focused onto the target with a set of electrodes that serve to further distance the positrons from the remnant magnetic field and provide the final focus.

First Phase: Beam focus on the remoderator foil

In order to extract the positron beam from the magnetic field we use a Mu-metal cup that we place over the solenoid magnet. This Mu metal cup has a 3 mm aperture on the beam axis and is used to terminate the magnetic field more rapidly than the $\sim z^{-3}$ decay of the solenoid. In the process of extracting the beam from the magnetic field, the positrons gain a significant amount of transverse energy, and the beam becomes diverging. In order to focus the beam we use a grid lens placed 10 mm from the mu-metal aperture. The grid has 200 lines per inch and is 90% transmitting. The grid lens efficiently compensates for the increased transverse energy gained in the magnetic field extraction as well as minimizes the chromatic aberration due to the buncher.

We used Simion 7.0 to trace the positron trajectories in our specific geometry. We also imported the magnetic field lines as calculated by the Poisson Superfish program to simulate the solenoid magnet and the Mu-metal termination. A typical Simion run is shown in Figure 10 where the envelop of the beam was traced.

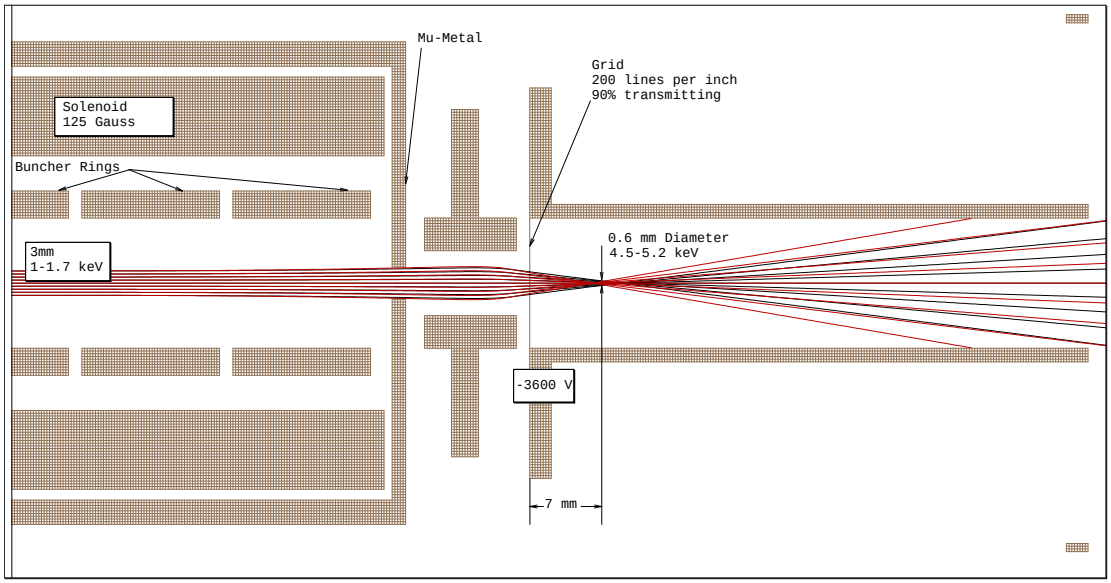

Figure 10 Simion simulation of the grid lens focus. The initial beam is 3 mm in diameter with 1-1.7 keV and is focused onto a 600 micron spot at 4.5-5.2 keV energy

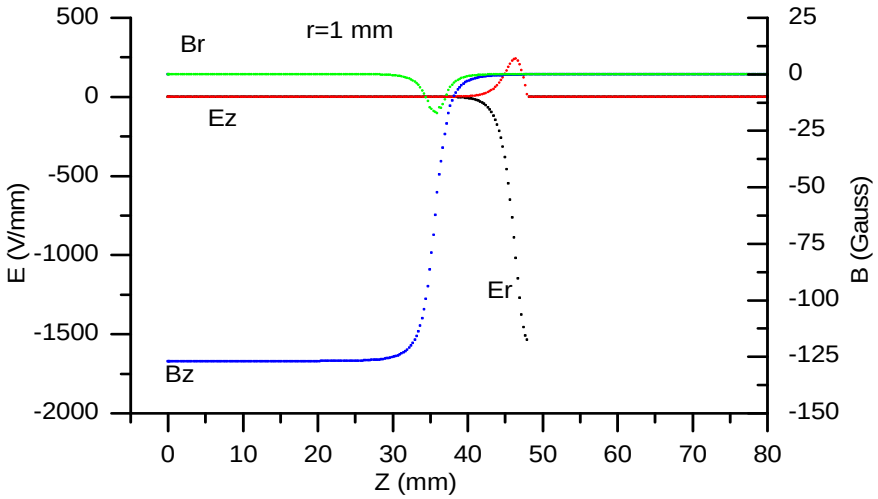

Figure 11 Electric and magnetic field in the longitudinal and radial direction 1 mm off-axis used for the focusing in the previous figure.

As a result of these simulations it was determined that the limiting factor is the energy spread due to the buncher. This energy spread leads to some chromatic aberration when the beam goes through the lens. Figure 11 shows the electric and magnetic field, both in the longitudinal and transverse direction, used in the Simion simulation shown in Figure 10.

Figure 10 shows the envelope of the beam and does not carry any beam density information. Simion allows us to create our own distribution and extract the resulting focused distribution. The beam spatial distribution was generated using the Box Muller generating function in order to obtain two coordinate normally distributed around the beam axis,

$$X = -2\ln U_1 \cos 2\pi U_2$$
$$X = -2\ln U_1 \sin 2\pi U_2$$

where U_1 and U_2 are two independent uniformly distributed random numbers from 0 to 1.

We flew 10 000 positrons in the optics drawn in Simion and recorded their initial and final position. We can simulate a CCD picture by binning the data from Simion in a 2D Matrix. In this simulation the pixels are 90 microns squares. Figure 3 shows a simulated image of the beam distribution used to represent the bunched beam before and after being focused.

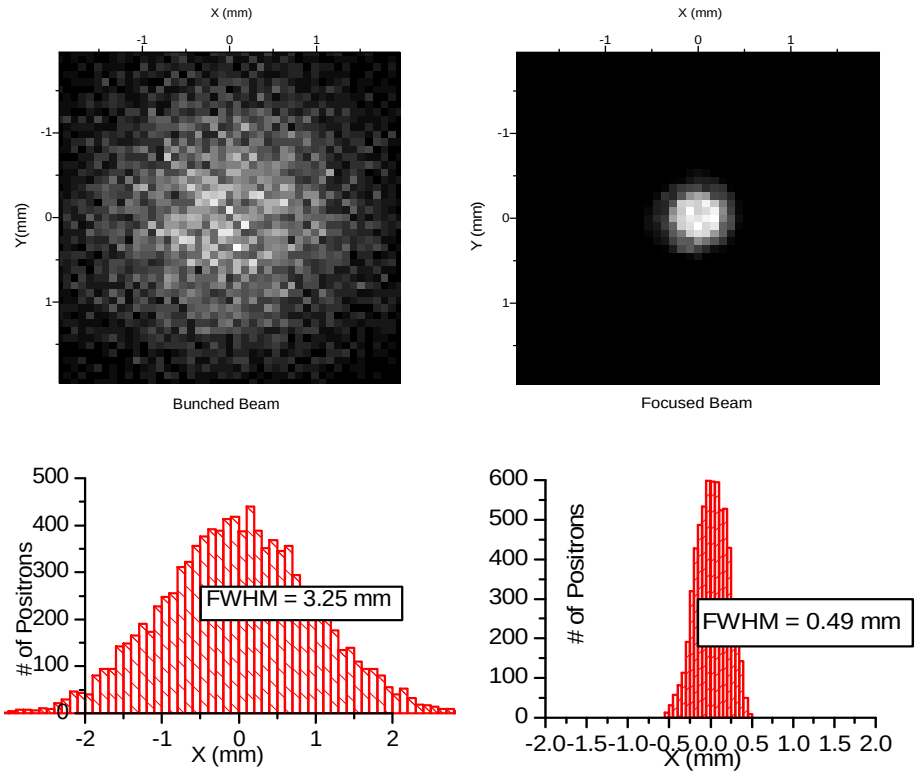

Figure 12 Image simulation of the bunched beam before and after going through the grid lens

Second Phase: Focus on the target

For the second set of electrodes we can use Liouville's theorem to estimate the final spot size from our initial beam parameters. Liouville's theorem states that in a conservative field the phase space remains constant. For an electrostatic beam this relationship can be written:

$$\Gamma = r\theta\sqrt{E} = const.$$

where r is the radius of the beam, θ is the pencil half angle, and E is the energy of the positrons.

The re-emitted positrons have a thermal transverse energy that goes like kT. We can then re-write Liouville's relation as $r_f = \Gamma / \theta_f \sqrt{E_f}$. To avoid aberration problems we keep θ_f <200 mrad.

Figure 13 shows a plot of the final spot size vs the final energy for different filling factors of the lens. We note that the spot size is reduced as the filling factor, hence the pencil half angle, is increased, however spherical aberration will limit the size of the final spot. In practice we try to keep the filling factor bellow 50%. This calculation can serve as a best case scenario target for the final focus.

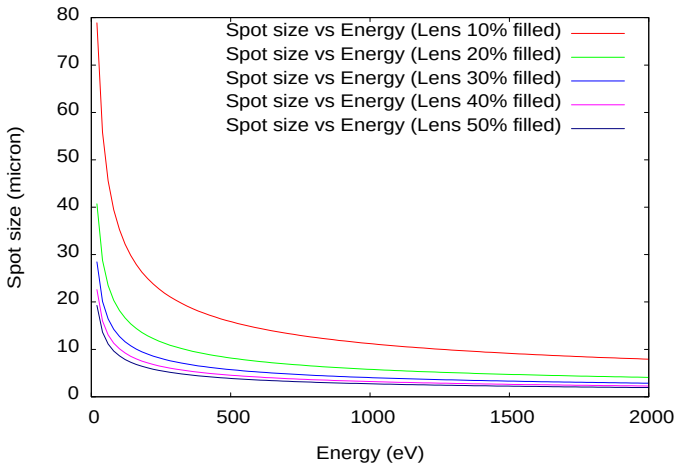

Figure 13. Final spot size vs final Energy for several lens filling factors.

The final set of electrodes can be separated in four stages:

- The Soa positron gun used to extract the positrons from the foil and accelerate them close to the target energy.
- The first Einzel Lens used to make corrections to the positron trajectories after coming out of the Soa gun and insure a parallel beam.
- The transfer tubes used to transport the positrons to the target. The first transfer tubes is equipped of four deflecting electrodes that can be used to correct for the effect of stray field in the transfer to the target.
- The second Einzel lens which provides the final focusing on the target.

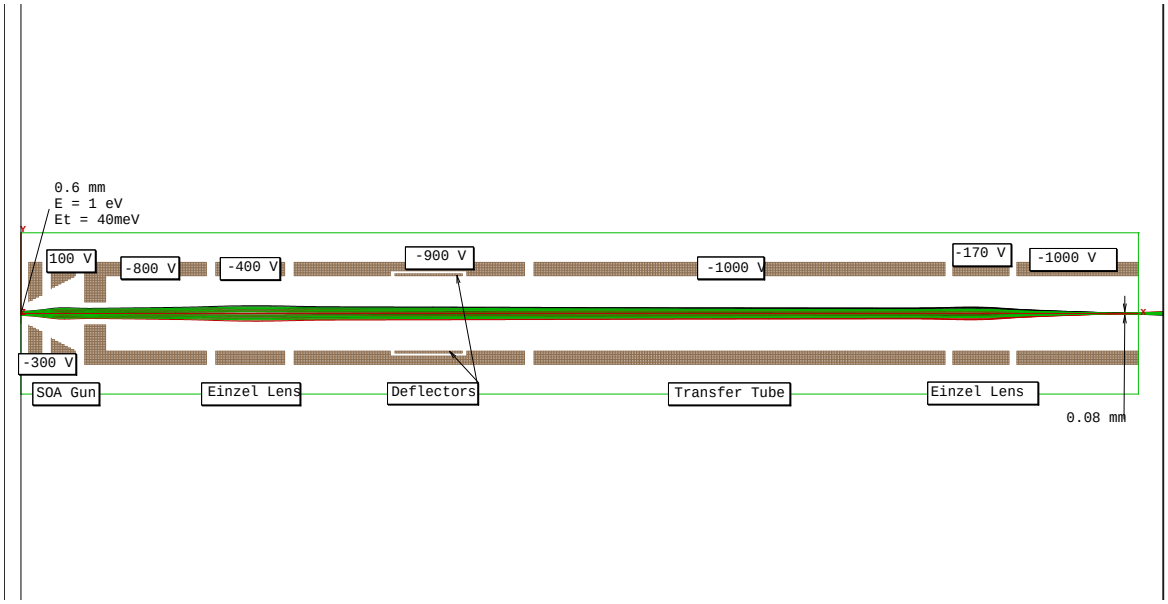

Figure 14 Second set of electrodes used to focus the beam on the target.

Figure 14 shows the geometry used for the second set of electrodes as well as a typical beam envelop. The best focus is achieved by carefully tuning the lens and reduce the effect of aberration. Once again it is

useful to look at the beam distribution at the target using a similar method as previously used.

This time 10,000 positrons are generated with a gaussian spatial distribution (FWHM 500 micron) and a thermal transverse energy set at 40 meV (gaussian in shape). We can simulate the result of a picture taken by the CCD camera as performed earlier (See Figure 15). Image resolution was increased to 2 microns per pixel for the final spot since the whole spot would fill one 90 micron pixel. The results of the simulations are shown in Table 1.

Table 1. Results from the Simion simulations with 10 000 positrons.

	FWHM initial	FWHM Focused	Energy spread initial	Transverse Energy initial	Final Energy
Grid Lens	3.25 mm	0.49 mm	700 eV	40 meV	4.5-5.2 keV
Canter's lens	0.49 mm	0.020 mm	40 meV	40 meV	1 keV

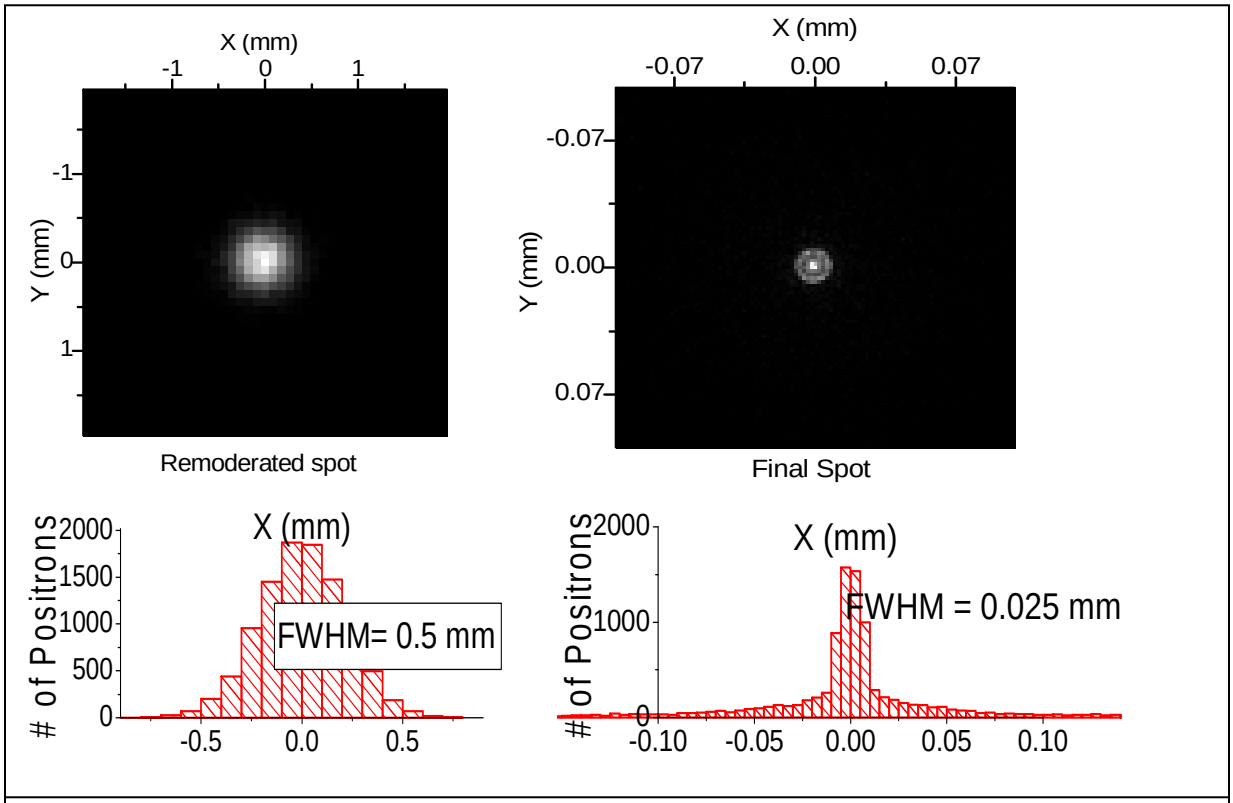

Figure 15. Results from the Simion simulations with 10 000 positrons.

II. Development of Laser systems

Various laser systems are under development for a variety of applications, including Ps laser cooling and Ps_2 spectroscopy. Many of the components have dual application.

Continuum Surelite 1-20 and Surelite Harmonic Generators

Two Surelite 1-20 Harmonic Generators SHG-I and THG. These nonlinear crystals in the SHG-1 is a type I nonlinear crystal and the THG is type II and each one produces 532 and 354.7 nm light by nonlinear frequency conversion of 1064 light from the Surelite 1-20. Characterization of the 1064 nm and SHG and THG mode was observed and also the power was measured for different q-switch delay times. The specifications of the 1064nm pulse are 8.4W with 420 mJ/pulse at 20Hz with a 6.59 ns time width. The 1064's collimation was measured by taking the burn pattern in 0.5m intervals from the head to 5.5 m. The top hat profile had a diameter that increased by a factor of two at around 5.5-5.0 m from the laser head and the uniformity of the mode degrades at 5.0m meters and beyond. It was also observed that the frequency of the xenon flash lamp in the Surelite 1-20 had to be operated at a frequency of 20 Hz. If a lower rep rate was chosen then the location of the waist, which was commercially positioned to be at the location of the harmonic generators, would change due to thermal lensing and the degree of collimation would go down at the SHG site and the mode of the SHG would change to an elliptical mode and affect the performance of the laser. The 532 will output around 2.0 W with 4-6 ns time width. The 355nm will output around 1.2W, 60mJ/pulse, with a 4-6 ns time width. Adjusting the back mirror for alignment of the YAG laser was done for both high power and good mode.

Alexandrite laser, PAL 101

A custom made Alexandrite laser was purchased from Lightage. Work and additional components were done and added by Dr. Wallying to meet the specification of the experiment to output 500 mJ of 729nm light, at 5Hz, with approximately 300ns time width. The threshold flash lamp voltage was measured around 729nm. The threshold voltage changes dramatically as the birefringent tuner is adjusted from 729 to within ± 3.0nm. Also the threshold voltage will decrease as you tune to the middle of the gain curve. Calibration for the Alexandrite laser is being verified and other behavioral aspects are currently explored and measured.

Optics

Four beamsplitters, CVI Higher High energy harmonic separators for separation of the 355, 532, and 1064nm light from the Surelite 1-20 were obtained. Six Beam Blocks/Dumps were made from double edge platinum razor blades. Two, AR coated for 532.1064 nm on both sides, BK7 Plane laser windows for the window cell for the nonlinear BBO crystal that doubles 1064 to 532 was bought. The manual specifications were incorrect and the Surelite's THG output is horizontally polarized light since the reflection from the surface of a pellin broca prism mounted at Brewsters angle was nearly diminished, so as a result a fair amount of 355 was reflected. A half wave plate made of quartz AR coated for 355nm with a 0.5" diameter in a 1.0 inch mount was purchased $305. A one inch rotational mount for the half wave plate was purchased. A Brewster Window Suprasil was used for input for vertically polarized 354.7 and 772nm from the dye laser. Please note that a custom dual AR coating for these wavelengths is very expensive so a Brewster window was substituted for a cheaper alternative. A plane laser window made of fused silica AR coated for 248 nm, $200. A fused silica plane convex lens with a focal length of 128.8 mm and a fused silica plane concave lens for 64.4 mm to telescope the 355 nm beam diameter down to improve the conversion efficiency of the sum frequency process. A plane window made of BK7 with a 1.0

inch diameter was cut into two equal semi circle pieces using a diamond tipped band saw and adjusted in height to produce a transparent platform that the BBO crystal could sit on to prevent ablation of the inner walls of the cell. Wax was used to stick the optic onto a thin glass plate that holds the optic as it was pushed slowly into the diamond saw since the thickness of the optic is 0.25 inches. A beaker of toluene was heated to a certain vapor pressure so that the residual wax could be taken off the glass platform. A mixture of 3:1 sulfuric acid and hydrogen peroxide was mixed in a Teflon beaker in a fume hood to clean the BK7 glass platform and the Brewster window for approximately an hour. The machined aluminum cell for the BBO crystal was placed in a soapy bath once and then an Ethyl alcohol bath twice for 30 minutes each in an ultrasonic bath with the heater on. The combined optical cell system that generates UV light was assembled in a grab bag purged with Helium gas. A Picomotor Newfocus Closed loop motorized stage was purchased to tune the 243nm and 250.9 nm light simultaneously with the dye laser and this work is currently in progress.

Dyes

A Dye was purchased for generation of 486 nm light. Two grams of Coumarin 500 were bought. One gram of LDS 765 was also bought to produce 772 nm light. The process of weighing using wax paper and extracting technique to weigh roughly 68 grams of LDS 765 to produce the proper molar concentration was done at least once using a high resolution weighing scale from another lab.

Electronics

Two NTE 1749 chips and a constant current power supply is borrowed form another lab was used to operate a stand-alone stepper motor attached to the PDL-1 dye laser. A basic unipolar 200 step 5.0 V 1.0 A stepper motor was examined. A labview program was made to program the stepper motor and the program can now tune the PDL-1 dye laser. The first NTE 1749 chip burned out since we wanted to see the upper limit of the tuning speed. A circuit was made that uses the NTE 1749 chip and connected to the power supply and the SCB-68 connector block from Labview. The DAQ board (NCI-6221) interfaced with a computer. A thermal couple was attached to the SCB-68 connector block and the thermocouple's temperature output was calibrated from numerous times using three known temperatures with an electronic thermometer. The Labview programmed thermocouple was then used to monitor the temperature of the NTE 1749 chip since there was no heat sink designed onto the board and an average of 0.5 amps drawn from the power supply could possibly damage the chip. But the temperature was observed to be 40 deg C for approximately seven hours of tuning the PDL-1, which is well below the upper limit of the temperature threshold of 125 deg C. A preprogrammed VI from Labview that performs temperature control was used to heat a cubic block of aluminum at 90 deg F using a 75-ohm resistor and the program maintained the temperature at 90 deg F with an inaccuracy of ±1.0 deg. The thermocouple was observed to have an accuracy of ± 1.0 deg C. A labview program was made to detect the line profile of the 632.816nm light using the stepper motor and labview program and the upper limit of the resolution of the 0.75m Czerny-Turner spectrometer was detected for second order. Currently the PDL-1 dye laser is also being tuned with the SCB-68 connector block.

Characterization/ Tuning/ Calibration of 0.75 m Czerny Turner Spectrometer

The Czerny Turner spectrometer that is made from SPEX and has two slits, two spherical metal mirrors, and one diffraction grating with 1200 lines/mm that is 10 cm by 10 cm large were all arranged in Czerny Turner geometry was borrowed from Professor Tom's group. Ken James started initial work that was done on the spectrometer. Adapters/mounts/ shafts/ spacers were machined by Ken James to adapt a Lin engineer stepper motor, that was purchased to the spectrometer. The original SPEX stepper motor burned

out. An optical encoder was used to tell the stepper motor to stop at the home position. We found a slope value for the 0.75 m spectrometer using the first and second order of the He-Ne line, 632.816 nm. The spectrometer has a nonlinear behavior between the dial number and the angle the grating rotates. But the output wavelength was found to have a one to one correspondence between the dial number/ wavelength reading and the output wavelength after looking at the geometry of the SPEX meter and observing the relationship between the incident angle, diffracted angle, incident angle and the rotated angle, diffracted angle and the rotated angle, and using the diffraction grating equation and observing that the mechanism of the SPEX spectrometer. The calibration was measured using a local slope using the output wavelength with the dial number. The spectrometer was extrapolated to have 0-1430 nm range for first order. A nitrogen laserwas used for the calibration since using the two sources of 1^{st} and 2^{nd} order of He-Ne located very far from the 243 location. Then calibration was done using the zeroth and 1^{st} order of 337.1 nm but that also was to far from 243 and also manually adjusting the spectrometer from a reference source could lead to inaccuracies of the set position for 243nm output and the resolution of 243 first order was less than ideal. A combination of 3^{rd} order 337.1 and 354.7nm was then found to provide a more accurate position and resolution by using the 4^{th} order of 243nm. An analysis was done what the upper limit of performance of the 0.75 Czerny-Turner spectrometer could achieve. Looking at the available sources and the wavelengths that were produced I recognized that we could use the 4^{th} order to get high resolution and accuracy.

Spectra Physics PDL-1 Dye laser

The dye laser was purchased from Anderson laser. A dye laser is a very cheap solution to obtain tunable wavelengths at high pulse powers. The pulsed laser system was characterized and achieved lasing by Ken James. The mode was modified to produce a near gaussian profile. Ken James then trained me in the following procedures. Ken James instructed the user on how to force the mode of the Dye laser into a TEM 00 mode by inserting a circular aperture inside the resonator of the PDL-1. Ken James also taught the proper recipe and mixing procedure for producing the Dye solution. Finding the correct concentration by performing a power optimization on the PDL-1 where the input light to the main amplifier is measured and modifying the concentration so that the amplifier is transmitting 10% of the input beam. We found that the oscillator concentration more sensitive compared to amplifier concentration. Identifying whether the mode is outputting amplified spontaneous emission, ASE, was also observed. The ASE will degrade the power output from the dye laser and we visually detected ASE from the coherence in the output or by using a dispersing optic such as a prism and observed the transmission of the final output of the dye and looked for the two wavelengths. If two are emitted then the lasing is in ASE. Ken also instructed me to achieve lasing by using two mirrors to control the direction on the input. Systematic procedures were practiced to optimize the alignment to produce good mode and power. Also the various dyes were looked at and the proper concentrations are readily achieved through documentation from Exciton. Ken also taught proper exchange procedures and cleaning process to the user. The gain vs. frequency was also measured for LDS 765.

243 nm light

A BBO crystal 6*6*10 mm AR coated for both sides to accept 355 and red was cut at 52.1 deg which was purchased for another phase of the experiment was found to be able to produce 243 nm light by using the SNLO program to see the correct phase matching angle and also double checked analytically. Other available crystals inside the Spectra Physics WEX in another lab are made of KDP so are not as efficient as BBO and are hygroscopic and more sensitive to temperature changes. The BBO was used. A cell was machined to hold the BBO that has a Brewster window input and a static seal and mounted adjustable platform to tune z and x-axis of the crystal. The combined system is now on an adjustable rotational stage along the axis. Two pinholes are used to align collinearly the 354.7 and the 772 nm pulses and also align

the BBO crystal face to reach the phase matching angle. The 354.7 nm was temporally detected with respect to the 772 nm dye output. The 354.7 nm was then time delayed around 10ns. Optimized spatial and temporal overlap of the 354.7 and 772 nm was achieved. Then a telescoping system was purchased to shrink the beam by a factor of two. Damage threshold values for the BBO were calculated for the BBO at the surface and these values were compared to published values to avoid surface or bulk damage to the BBO with multiple shots of 354.7 and 772. A beam diameter of around 3mm was reach for the 354.7 nm light and a few factors down from the AR coating damage threshold upper limit. Theoretical values of the conversion efficiency were calculated. Values for the 2^{nd} order nonlinear coefficient was also obtained from published values and deff for the BBO at 49.8 deg was obtained. The power of the 243nm was measured. After alignment of the BBO crystal the crystal was found to rotate from 52.1 deg to 48.3 deg to produce SFM of 243 nm light. The 243 nm pulse was measured using the 0.75 spectrometer. Characterization of the tunability of the 243 nm was also studied while manually rotating the grating on the PDL-1. The temporal profile was monitored and optimum phase matching angle was explored. The 243nm pulse is capable of around 1.4 mW of 243 nm light. The tuning procedure is currently where most of the focus is, and we are currently focusing on tuning the range on the order of Terahertz. The pulse width is around 4-5ns and the line width was measured to be around 60 Ghz with a limiting spectrometer resolution of 0.0021nm / 10.6 Ghz.

Second Harmonic 532 ionizing pulse

Another cell was machined to hold a BBO crystal cut at 22.9 deg with 8×8×8 mm^3 dimension. The cell has a static seal in a helium buffer gas with two windows made of BK7 that are AR coated for both 1064 and 532 nm light and is mounted on an adjustable platform for the phase matching angle and a second axis is also adjustable. The same cleaning procedures were used to clean the cell as in the SFM 243nm cell. Two pinholes are used to align the 1064nm light that is coming from the leftover 1064 that was used to produce 532 and 355nm light from the Surelite 1-20. Visual indication of surface damage was examined shot to shot since the Surelite 1-20 is outputting relatively high power.

Optical Layout

The optical table is 4 by 10 feet. An efficient layout of the laser's and optical components was achieved that provides access to either side of the positron beam line. We have arranged the optical components to produce sum frequency mixing of 354.7 and 772 to produce 243 nm light with the 354.7 time delayed for 10ns. Also the leftover 1064 can be is being converted to 532 with a time delay and separated safely. The 1.0m and 0.5 meter spectrometer can be used simultaneously with the Alexandrite laser and room is available in front of the Alexandrite laser to perform future diagnostics.

Enclosure/Filtration Room

An enclosure was built with an air filtration system and cooling system. The 243 beam is separated by a pellin broca prism and fired outside the enclosure. Beam tubes are currently used to guide the 243 nm outside the enclosure and into one of the vacuum chambers for laser safety reasons.

Linewidth Detection

The 243 nm was sent through the spectrometer and we attempted to take a single shot burn pattern at the exit aperture using laser paper. Also fluorescent chalk placed on paper substituted for the laser paper. Both did not work. A UNIQ CCD camera with an EPIX imaging board, which were borrowed from Professor Tom's group was then installed. The hardware issues are not quite resolved but we imaged the 632.816

nm light from a He-Ne laser, the 337.1 nm light from a nitrogen laser . The 3rd and 4th order of the Nitrogen laser line was imaged. The 4th order was found to have a higher resolution which verifies the theory behind the upper resolution limit of the spectrometer. The 243 linewidth images can also be measured using software and that work is currently in progress.

Figure 16. Linewidth Detection of three different 243 nm single shot on to a CCD camera. Please note the halo around the center of the rectangular image is due to fluorescence. The position of each shot did not move as we observed in realtime the shot to shot stability. The size and scale of the image is the same for each shot.

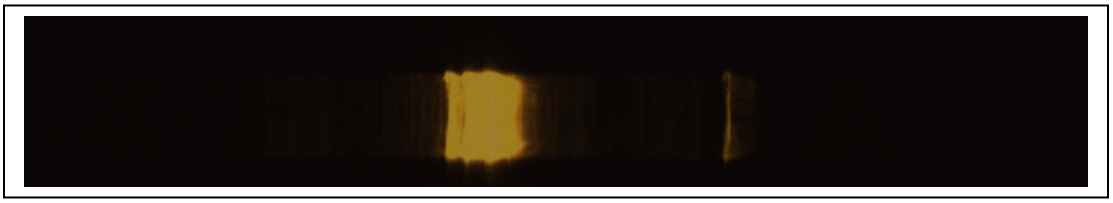

Figure 17. 337.1 nm single pulse detection at using the 3rd order of the Spectrometer.

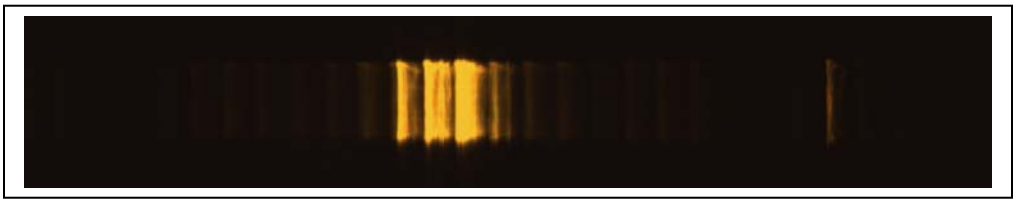

Figure 18. 337.1 nm single pulse detection at 4th order. Please note the size and scale the image in this and the previous figure are the same.

III. Preliminary estimate of ignition of a DT reaction using a 1 MJ annihilation gamma ray laser pulse.

The nucleon number density is nN where *N* is the factor the density has been increased above liquid number density $n = 5\times10^{22}\,cm^{-3}$.

The initial temperature is *kT*, the initial energy deposited a spherical cylindrical plasma is [Note that the follosing formulae are highlighted in green or blue to correspond to conditions where the starting point is spherical or cylindrical respectively.] $E = \frac{3}{2}kT\,2nN\Omega$, and the volume is $\Omega = \frac{4}{3}\pi r^3$ $\Omega = \pi r^2 l$. The factor 2*nN* gives the total number density of particles in the plasma, ions plus electrons.

$$E = 3nN\Omega kT = 3\times5\times10^{22}\times N\times\tfrac{4}{3}\pi\times10^{-6}\times2\times10^{4}\times\left[\frac{r}{0.01cm}\right]^3\times\left[\frac{kT}{20keV}\right]\times1.6\times10^{-19}\,J$$

$$=\left[\frac{N}{10}\right]\times\left[\frac{kT}{20keV}\right]\times\left[\frac{r}{0.01cm}\right]^3\times20kJ$$

$$E = 3nN\Omega kT = 3\times5\times10^{22}\times N\times\pi\times10^{-6}\times2\times10^{4}\times\left[\frac{r}{0.01cm}\right]^2\times\left[\frac{l}{3mm}\right]\times\left[\frac{kT}{20keV}\right]\times1.6\times10^{-19}\,J$$

$$=\left[\frac{N}{10}\right]\times\left[\frac{kT}{20keV}\right]\times\left[\frac{r}{0.01cm}\right]^2\times\left[\frac{l}{3mm}\right]\times450kJ$$

The speed of the expanding heat front is $\langle v\rangle = c\sqrt{\frac{3kT}{M_{DT}c^2}}$.

The average reaction yield will be the thermally averaged sigma-v product at 20 keV, $\langle\sigma v\rangle = 4.2\times10^{-16}$ cm^3/s times the number density times the interaction time *dt* or

y = $n\langle\sigma v\rangle N dt$.

The locally deposited energy *dE* is due to one alpha particle with energy ε=3.5 MeV per DT reaction, or

$dE = \frac{1}{2}\varepsilon n^2\langle\sigma v\rangle N^2\Omega dt$, where $dt = dr/\langle v\rangle$

To first order in *dt* the change in temperature after an interaction time *dt* will be

$dT = T(dE/E - 3dr/r)$ $dT = T(dE/E - 2dr/r)$.

Rewrite this as $\frac{dT}{T} = \frac{dE}{E} - 3\frac{dr}{r} = \frac{\frac{1}{2}\varepsilon n^2\langle\sigma v\rangle N^2\Omega dt}{\frac{3}{2}kT\,2nN\Omega} - 3\frac{dr}{r} = \frac{\frac{1}{2}\varepsilon n^2\langle\sigma v\rangle N^2\Omega dr}{\frac{3}{2}kT\,2nN\Omega\langle v\rangle} - 3\frac{dr}{r}$.

$$\frac{dT}{T} = \frac{dE}{E} - 2\frac{dr}{r} = \frac{\frac{1}{2}\varepsilon n^2\langle\sigma v\rangle N^2\Omega dt}{\frac{3}{2}kT\,2nN\Omega} - 2\frac{dr}{r} = \frac{\frac{1}{2}\varepsilon n^2\langle\sigma v\rangle N^2\Omega dr}{\frac{3}{2}kT\,2nN\Omega\langle v\rangle} - 2\frac{dr}{r}$$

For 15<*T*<30 keV, $\langle\sigma v\rangle \approx \sigma(T)\langle v\rangle = (T/10keV)^{3/2}\times1.5\times10^{-16}\,cm^3s^{-1}$, as is evident from Figure 19. We then have

$$\frac{dT}{T}=\frac{\varepsilon n\langle v\rangle\sigma(T)Ndr}{6kT\langle v\rangle}-3\frac{dr}{r}=\left[\frac{\varepsilon n(T/10keV)^{3/2}\times1.5\times10^{-16}cm^3s^{-1}\sqrt{M_{DT}c^2}Nr}{6kT\sqrt{3kTc}}-3\right]d\ln r=$$

$$\left[\frac{\varepsilon}{10keV}\frac{5\times10^{22}cm^{-3}\times1.5\times10^{-16}cm^3s^{-1}\sqrt{M_{DT}c^2/10keV}Nr}{6\sqrt{3}c}-3\right]d\ln r=$$

$$\left[\frac{3500keV}{10keV}2.5\times10^{-5}cm^{-1}\sqrt{2{,}300{,}000keV/10keV}Nr-3\right]d\ln r=$$

$$\left[7.5\times10^{-3}cm^{-1}\sqrt{230{,}000}Nr-3\right]d\ln r=$$

$$\left[3.75cm^{-1}Nr-3\right]d\ln r=\left[3.75\left[\frac{N}{10}\right]\left[\frac{r}{1mm}\right]-3\right]d\ln r$$

$$\frac{dT}{T}=\frac{\varepsilon n\langle v\rangle\sigma(T)Ndr}{6kT\langle v\rangle}-2\frac{dr}{r}=\left[\frac{\varepsilon n(T/10keV)^{3/2}\times1.5\times10^{-16}cm^3s^{-1}\sqrt{M_{DT}c^2}Nr}{6kT\sqrt{3kTc}}-2\right]d\ln r=$$

$$\left[\frac{\varepsilon}{10keV}\frac{5\times10^{22}cm^{-3}\times1.5\times10^{-16}cm^3s^{-1}\sqrt{M_{DT}c^2/10keV}Nr}{6\sqrt{3}c}-2\right]d\ln r=$$

$$\left[\frac{3500keV}{10keV}2.5\times10^{-5}cm^{-1}\sqrt{2{,}300{,}000keV/10keV}Nr-2\right]d\ln r=$$

$$\left[7.5\times10^{-3}cm^{-1}\sqrt{230{,}000}Nr-2\right]d\ln r=$$

$$\left[3.75cm^{-1}Nr-2\right]d\ln r=\left[3.75\left[\frac{N}{10}\right]\left[\frac{r}{1mm}\right]-2\right]d\ln r$$

and

$d\ln T=adr-3d\ln r$. $d\ln T=adr-2d\ln r$

The solution is $\ln T/T_0=a(r-r_0)-3\ln r/r_0$ or $T/T_0=(r_0/r)^3\exp\{a(r-r_0)\}$, where for N=10, a = 37.5 cm^{-1}. The deposited energy required for ignition at T_0= 20 keV is about 0.5 MJ for an initial plasma radius of 300 μm.

The solution is $\ln T/T_0=a(r-r_0)-2\ln r/r_0$ or $T/T_0=(r_0/r)^2\exp\{a(r-r_0)\}$, where for N=10, a = 37.5 cm^{-1}. The deposited energy required for ignition at T_0= 20 keV is about 2 MJ for an initial plasma radius of 200 μm. See Figure 20.

By the time the burn has expanded to 3 mm radius, the energy yield will be 5 GJ or 1 ton of TNT, about 1% of the energy needed to make the positrons for a 0.5 MJ gamma ray burst.

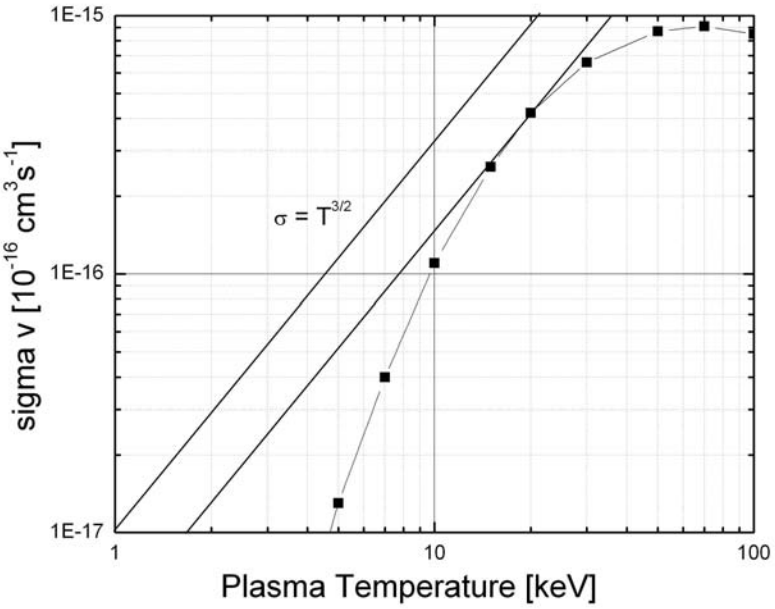

Figure 19. Sigma-v product as a function of plasma temperature for a DT mixture.

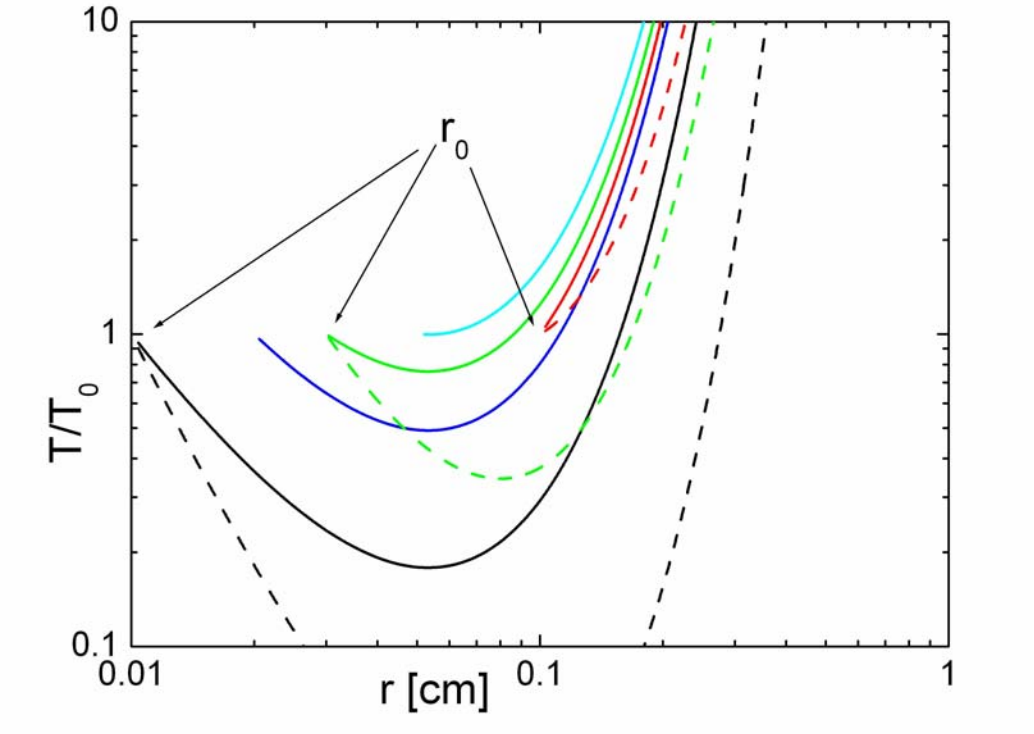

Figure 20. Plasma temperature as a function of its radius for an expanding DT burn starting at radius r_0 and temperature $T_0 \approx 20$ keV. The dashed lines are for spherical burns, while the solid lines are for cylindrical burns.

IV. New method for cooling positronium

Laser-cooling laser system: *Design considerations*

- Wavelength should be 243 nm resonant with the triplet 1S-2P transition
- Pulses should have constant π-pulse fluence of 1.6 nJ/cm2/50 MHz where 50 MHz is the natural linewidth. The spectrum of the cooling pulse should have a flat-top intensity distribution set at this fluence.
- Repetition rate should be the triplet 1S-2P spontaneous lifetime 3.2 ns
- Pulse train should have 88 pulses over a duration of one annihilation lifetime. The triplet 1S ground state annihilation lifetime is 142 ns. Under high excitation rate the atom will spend half its time in the 2P state so the annihilation lifetime is doubled to 284 ns. There are 88 periods of 3.2 ns in 284 ns.
- Ps atoms are emitted from the surface of a 0.5 mm diameter moderator and the laser-atom interaction region is a 5 mm diameter Gaussian sphere centered 5 mm above the moderator. Only particles emitted in the solid cone with half angle 26.6 degrees need to be laser-cooled: the distribution in vz has double the velocity that is in ±vx and ±vy and thus the cooling laser beam in z must be twice the intensity as in x and y. The single-photon recoil results in a 6 GHz Doppler-shift so with 44 photons in the z-direction, we should be able to cool all velocity groups with redshifts between 0 and 264 GHz to the recoil limit of 6 GHz which corresponds to 0.6 K. The spectrum should have sharp edges at 0 and -264 GHz relative to line-center to avoid heating the ~0.6 K atoms and partial cooling of hotter atoms that should instead be allowed to rapidly exit the interaction region.
- The spectral energy density should be flat and stable across the 264 GHz bandwidth—this requires a means of locking the modes to avoid mode competition and unacceptable energy differences between the spectral components decelerating different velocity groups. A 1.2 ps 243 nm pulse has the right bandwidth. We choose to make this using a 2 ps transform-limited 729 nm pulse, then frequency-tripled to 243 nm.
- The Ps atoms are emitted from the moderator with a thermal tail at ~100 K which has a Doppler-width of 267 GHz full-width half-max. This matches the 264 GHz bandwidth of the laser-cooling pulse very well: 98% of the 100 K atoms spending enough time in the interaction region should be cooled to ~0.6 K.
- Laser-cooling is essential to the success of the high-resolution spectroscopy experiments because it reduces Doppler-broadening and transit broadening and can help increase the number of atoms participating in the measurement by stopping them in the interaction region. It must be reliable and nearly turn-key, easily monitored, changed, optimized, and controlled via computer, and stable for long periods of time up to 90 days. Substantial development time must be devoted to delivery of the laser-cooling beams in 3-dimensions in the interaction region and compensation for laser-power and thermal drifts in mechanical systems.

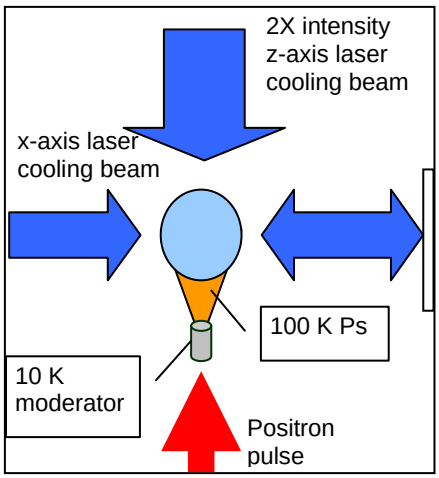

Figure 21. Laser cooling beams intersecting the Ps atoms.

Development Strategy: Design implementation (see schematic setup is shown in Figure 21).

- The single pulse will be amplified in the custom Ti:Sapphire ring-cavity regenerative amplifier which is shown in detail to highlight differences from the usual regenerative amplifier. The custom Ti:Sapphire ring-cavity regenerative amplifier will have two outputs controlled by 2 Pockels cells (PC) and thin-film polarizers (TFP) labeled #1 and #2. The Ti:Sapphire rod (Brewster cut and in a z-cavity to compensate for astigmatism) will be pumped with a 532 nm pulse derived from the second-harmonic output of a Q-switched Nd:YAG laser (Continuum PowerLite Precision II 9010) generating 1 J of 532 nm per pulse. The 532 nm nearly flat-top beam will be relay-imaged into the Ti:Sapphire rod in a 6 mm diameter spot to deposit 3 J/cm2 fluence and to produce an initial single pass gain of 2. A computer-controlled attenuator (using a waveplate on a rotation stage and polarizer) will compensate for drifts in the 532 nm pulse energy. Insertion losses are assumed to be 6% per roundtrip. PC 2 will fire full half wave voltage initially to trap the 729 nm pulse inside the cavity. The calculated intracavity pulse energy is shown in the upper panel of Figure 23 as a function of round trip number. After 26 round trips the pulse energy will reach around 12 mJ and then PC 1 and PC 2 will rotate the polarization to couple out a fraction on the order of 40% and 10% per pass. The control voltages on PC 1 and PC 2 will be varied in time over the next 300 ns to maintain a constant 5 mJ energy on output #1 and to dump energy through output #2 so the intracavity energy does build too fast and deplete the gain prematurely. Between roundtrips 26 and 126, the fractional outputs decrease monotonically and nearly linearly and this is the practical limit for precision control of the high voltages driving the Pockels cells. The peak intracavity energy pulse energy will only reach 42 mJ and in 10 ps duration with a Gaussian waist of 2.5 mm, the peak intensity would be 40 GW/cm2 which is below the 50 GW/cm2 limit for phase-distortion and potential for self-focussing.

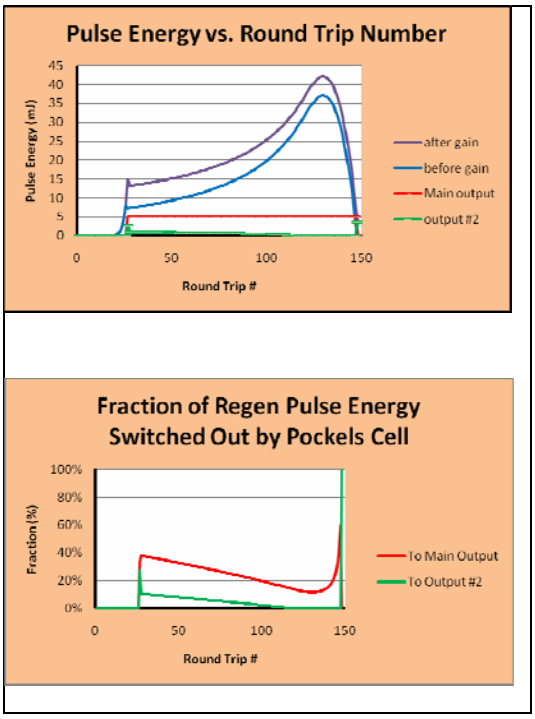

Figure 23. Upper: Pulse energy after each round trip for immediately out of gain medium, input to gain medium, the main output #1, and the secondary output #2. Lower: Fraction of intracavity pulse energy switched out on each round trip to the main output #1 and to output #2.

- We will design and fabricate our own custom high voltage amplifiers using planar triodes and use a Tektronics AFG3252 240 MHz arbitrary waveform generator to computer-control the drive voltages for the Pockels cell. The AFG3252 allows 12-bit voltages to be read out of memory at 0.5 ns intervals so the ~300 ns duration can be specified

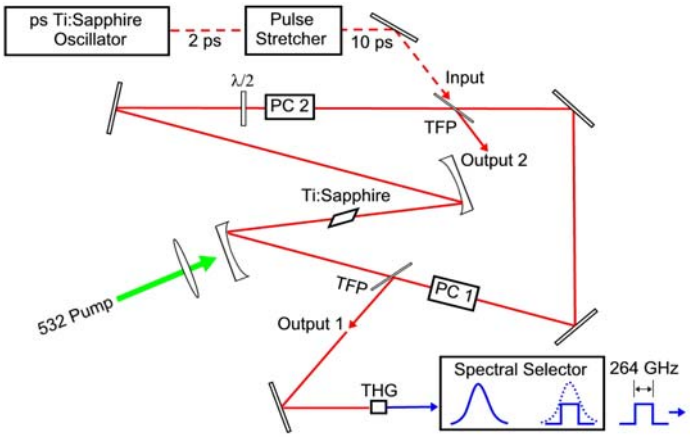

Figure 22. Schematic setup of Laser-Cooling Laser System

by as many as 600 points. The energy of pulses inside the cavity and the outputs will be measured on every pulse, and computer algorithms will be developed to use those measurements to continuously update models of the amplifier gain and loss parameters and update the optimized waveforms to drive the Pockels cells. This will compensate for thermal drifts.

- The 5 mJ, 729 nm pulses will be frequency-tripled in Type I/ II BBO to give 0.5 mJ, 243 nm pulses.
- The sharp red and blue cutoffs of the 243 nm spectra will be set with 6 GHz resolution by double-passing through a Martinez-style pulse "stretcher" employing two anti-parallel gratings and a 1:1 cylindrical lens telescope with f=1.5 m shown in Fig. 5. The beam focused through a 5 μm slit and then re-collimated to fill the first grating. At least 8 cm of the 2400 l/mm grating must be illuminated to obtain 6 GHz resolution in the focal plane between the cylindrical lenses of the 1:1 telescope. Hard apertures will be set to obtain the 6 GHz cutoffs roughly at the ½ heights of the spectrum and shown in Fig. 3. The gratings will be Al-coated 2400 l/mm (Richardson's 53-*-150R) with 70% reflectivity at 243 nm. After double-passing, the transmission will be 8% leaving 0.04 mJ/pulse.
- The spectrum will be made flat-top in intensity by passing through an anti-resonant etalon adjusted to provide 50% transmission at the peak and 100% transmission at the red and blue cutoffs with overall transmission ~60%. The expected energy output will be 0.024 mJ.
- The final output will have 0.024 mJ spread over 264 GHz, or 4.5 nJ/50 MHz. This exceeds the π-pulse fluence requirement of 1.5 nJ/cm^2/50 MHz.
- Development will include diagnostics of the oscillator (autocorrelation, spectrum, computer-controlled tuning), the pulse energies inside and extracted from the regenerative amplifier as a function of time and roundtrip number, computer control of the PC voltages, developing algorithms for optimizing the constant energy in the pulse train, and propagating the multiple beams from the laser table and enclosure into the positron beam vacuum chamber using piezo-controlled mirror mounts and quad-position detectors or other feedback signals to compensate for drifts. Laser amplitude drifts will be compensated computer-controlled attenuators using waveplates on rotation stages and polarizers.

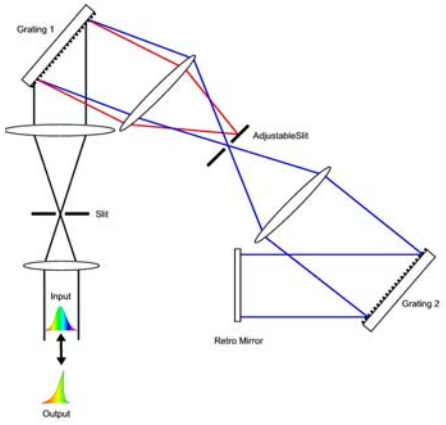

Figure 24. Spectral selection requires 6 GHz cutoffs in a spectrometer like geometry combined with pulse-shape reconstruction in a Martinez anti-parallel grating "pulse stretcher".

CONCLUSIONS

We have demonstrated progress in the production and utilization of positron pulses that can possibly be scaled up by four orders of magnitude to the point where we will be able to demonstrate stimulated annihilation. We have developed the lasers that will be useful for cooling and diagnostics as we attempt to make the first positronium Bose-Einstein condensate. We have also estimated that about 1 MJ would be required to initiate DT burn. Considerably more development would be required to achieve this goal.

RECOMMENDATIONS

Making a positronium annihilation gamma ray laser is really very simple in principal.

The required steps are (1) producing, trapping, storing, releasing, bunching, and focusing the positrons; (2) forming and cooling the triplet positronium in the correct geometry; and (3) switching the triplets to singlets at the desired moment.

Extrapolating from past progress in storing positrons [10^2 in 1984 to 10^{10} at present] it is evident that at the single investigator level it would be a decade before we would see the stimulated emission of annihilation radiation and a quarter century before we could make a MJ laser.

With about 10 times the effort the above times could probably be cut in half and one would know after 2-3 years whether there were any insurmountable roadblocks.

There are no advantages to using antimatter as an energy delivery mechanism if efficiency or total yield is a consideration because we know of nowhere to mine positrons or antiprotons.

However, if penetration, speed of delivery, leaving no trace, and micro-radian aiming precision are of concern, the gamma ray laser is paramount. Besides that, the possibility of using the laser as a trigger for actinide-free fusion hint at the solution to the world's energy problems and offer a way for us to defend the US without quibbling about fall-out.

Therefore it would seem that a 10x increase in the effort towards the gamma ray laser would be a reasonable investment at this time, with a further factor of ten increase or abandonment to follow depending on the results of a few years more development.

REFERENCES

[1] A. P. Mills, Jr., D. B. Cassidy and R. G. Greaves, "Prospects for making a Bose-Einstein-condensed Positronium Annihilation Gamma Ray Laser", *Materials Science Forum* 445-446, 424-429 (2004).

[2] D. B. Cassidy, S. H. M. Deng, R.G. Greaves, T. Maruo, N. Nishiyama, J. B. Snyder, H. K. M. Tanaka and A.P. Mills, Jr., Phys. Rev. Lett. 95, 195006 (2005).

[3] D. B. Cassidy and A. P. Mills, Jr., *Nature (London)* **449**, 195 (2007).

[4] C.M. Surko and R.G. Greaves, *Physics of Plasmas* **11** (2004) 2333.

[5] D. B. Cassidy, S. H. M. Deng, R. G. Greaves, and A. P. Mills, Jr., *Rev. Sci. Instrum*. **77**, 073106 (2006).

[6] D. B. Cassidy, S.H.M Deng, H. K. M. Tanaka and A. P. Mills, Jr., Appl. Phys. Lett. 88, 194105, (2006).

[7] D. B. Cassidy DB, S. H. M. Deng, A. P. Mills, Jr., Phys. Rev. A, **76** 062511 (2007).

[8] A. P. Mills, Jr. Nuclear Inst. and Methods in Physics Research, B 192, 107 (2002).

[9] C. D. Anderson, Phys. Rev. 43, 491 (1933).

[10] M. Deutsch, Phys. Rev. 82 455 (1951).

[11] A. P. Mills Jr., Phys Rev. Lett 46, 717 (1981).

[12] A. Wheeler, Ann. N.Y. Acad. Sci. 48, 219 (1946).

[13] A. P. Mills. Jr., Appl. Phys. 23 189 (1980)

DISTRIBUTION LIST
AFRL-RW-EG-TR-200X-7080

Defense Technical Information Center — 1 Electronic Copy (1 File & 1 Format)
Attn: Acquisition (OCA)
8725 John J. Kingman Road, Ste 0944
Ft Belvoir, VA 22060-6218

EGLIN AFB OFFICES:

AFRL/RWOC (STINFO Office) - 1 Hard (Color) Copy
AFRL/RW CA-N - STINFO Officer Provides Notice of Publication

AFRL/RWG - 1 Copy
AFRL/RWM - 1 Copy

STINFO COPY